World Academy of Science, Engineering and Technology
International Journal of Electrical and Computer Engineering
Vol:5, No:12, 2011

Mathematical Model and Control Strategy on DQ Frame for Shunt Active Power Filters

P. Santiprapan, K-L. Areerak* and K-N. Areerak

***Abstract*—**This paper presents the mathematical model and control strategy on DQ frame of shunt active power filter. The structure of the shunt active power filter is the voltage source inverter (VSI). The pulse width modulation (PWM) with PI controller is used in the paper. The concept of DQ frame to apply with the shunt active power filter is described. Moreover, the detail of the PI controller design for two current loops and one voltage loop are fully explained. The DQ axis with Fourier (DQF) method is applied to calculate the reference currents on DQ frame. The simulation results show that the control strategy and the design method presented in the paper can provide the good performance of the shunt active power filter. Moreover, the %THD of the source currents after compensation can follow the IEEE Std.519-1992.

***Keywords*—**shunt active power filter, mathematical model, DQ control strategy, DQ axis with Fourier, pulse width modulation control.

I. Introduction

Nowadays, nonlinear loads are widely used in industries. These loads generate harmonics into the power system causing a lot of disadvantages [1]–[4]. Therefore, it is considerable to reduce or eliminate the harmonics in the system. The shunt active power filter (SAPF) is the tool to solve the harmonic problem because this filter provides higher efficiency and more flexible compared with a passive power filter [5]. There are three main parts to be considered for using the shunt active power filter as shown in Fig. 1. The first is the harmonic detection method to calculate the reference currents of the shunt active power filter.

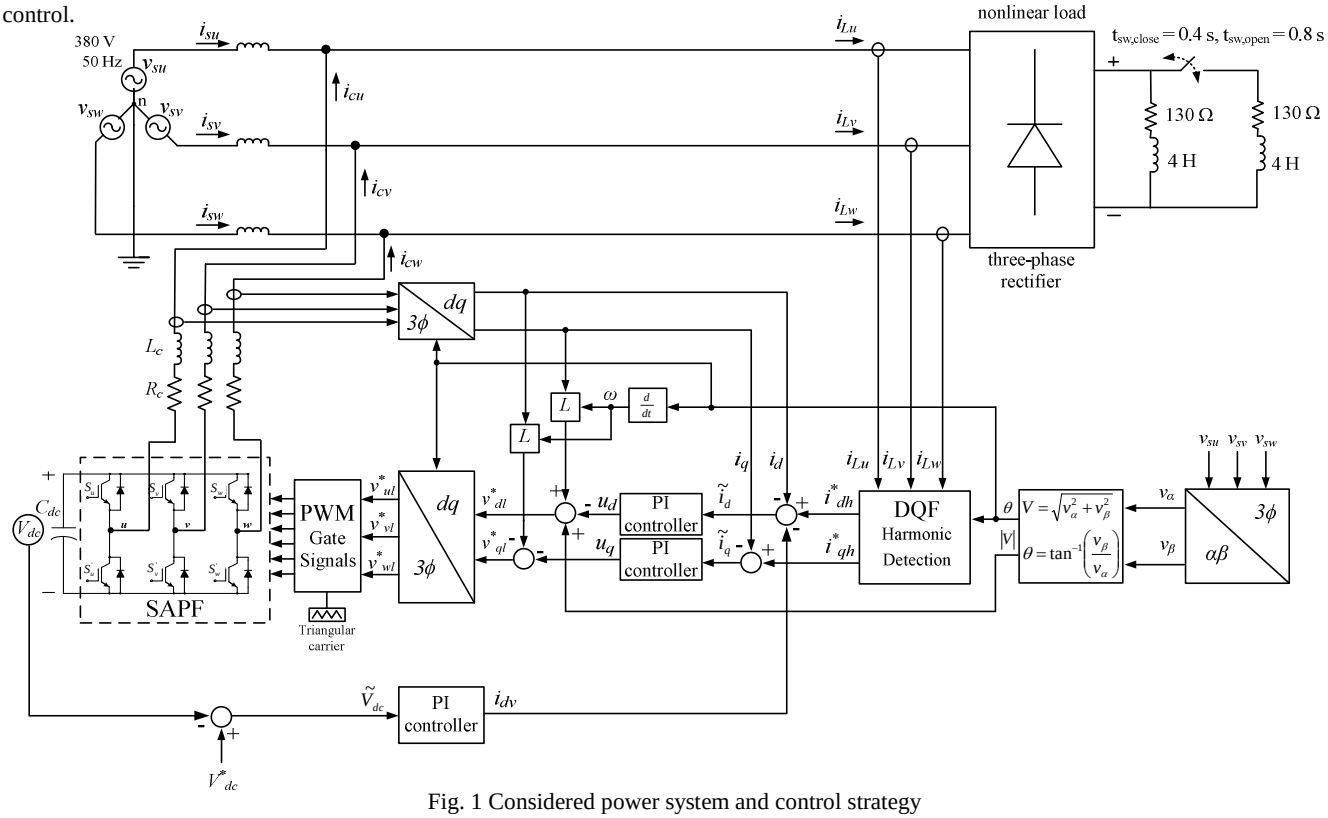

Fig. 1 Considered power system and control strategy

There are many methods to calculate the reference currents such as the instantaneous power theory (PQ) [6], the synchronous reference frame (SRF) [7], the a-b-c reference frame [8], the synchronous detection (SD) [9] and the DQ axis with Fourier (DQF) [10]. In this paper, the DQF is selected for the harmonic detection because this method provide the fast calculation time in which it is suitable for the real time application. The second part is the structure of shunt active

P. Santiprapan, master student in electrical engineering, PQRU Research unit, PeMC Research group, School of Electrical Engineering, Suranaree University of Technology Nakhon Ratchasima, 30000, THAILAND.

*K-L. Areerak, Assistant Professor, PQRU Research unit, PeMC research group, School of Electrical Engineering, Suranaree University of Technology Nakhon Ratchasima, 30000, THAILAND (corresponding author: kongpol@sut.ac.th).

K-N. Areerak, lecturer, PeMC research group, School of Electrical Engineering, Suranaree University of Technology Nakhon Ratchasima, 30000, THAILAND.

power filter. The voltage source inverter (VSI) with six IGBTs is used for the shunt active power filter. The last one is the control technique and control strategy to control the compensating currents (i_{cu}, i_{cv} and i_{cw}). There are many techniques to control the compensating currents such as the hysteresis current control [11], the delta modulation control [12], the fuzzy logic control [13] and the pulse width modulation control [14]. The pulse width modulation (PWM) with PI controllers on DQ frame is used in this paper as shown in Fig. 1. Therefore, the details of PI controllers design with the PWM technique for the current and voltage loops on DQ frame are presented.

The paper is structured as follows. The review of the DQF method is addressed in Section II. The mathematical model of shunt active power filter is fully presented in Section III. The designs of two current loop controllers and one voltage loop controller on DQ frame and control strategy are explained in Section IV and Section V, respectively. In Section VI, the simulation results and discussions are presented. Finally, Section VII concludes the work in the paper.

II. Review of The DQ Axis with Fourier (DQF) Method

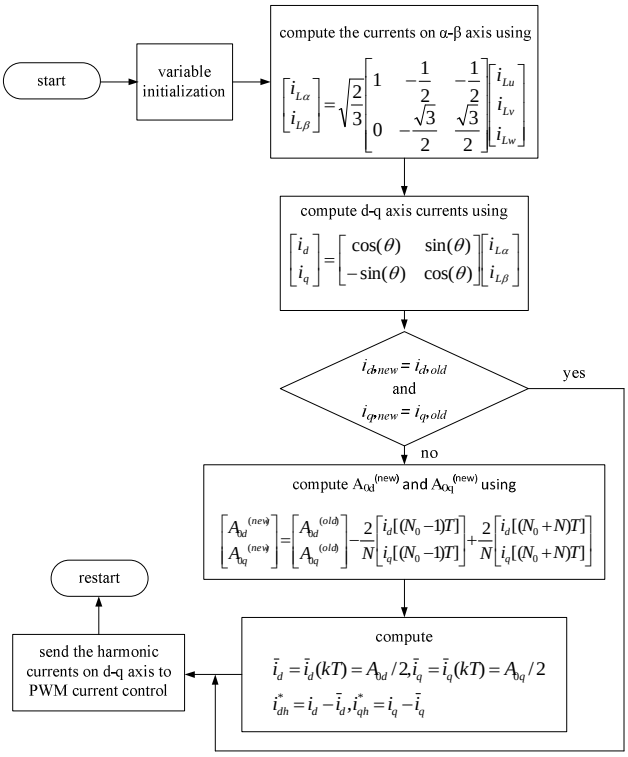

Fig. 2 Flowchart of the DQF method

The DQF algorithm is the excellent method to identify the harmonic in the power system. This method is a combination between the advantages of the synchronous reference frame method (SRF) [7] and the sliding window Fourier analysis (SWFA) [15]. The DQF method is firstly presented in 2007 by Sarawut Sujitjorn, Kongpol Areerak and Thanatchai Kulworawanichpong [10]. In 2007, the DQF method is operated with only the shunt active power filter to eliminate all harmonic components in the system. In 2008 [16], Kongpol Areerak extends the work in [10] to apply the DQF method operated with the hybrid power filter to eliminate some harmonic components depending on the engineering design. In this section, the detail of the DQF method to identify the harmonic current on the d-q axis in the system is presented. The flowchart of overall procedure to calculate the harmonic currents on d-q axis (i_{dh}^*, i_{qh}^*) using the DQF method is illustrated as shown in Fig. 2. The more details of the DQF method can be found in [10] and [16].

III. The Mathematical Model of Shunt Active Power Filter

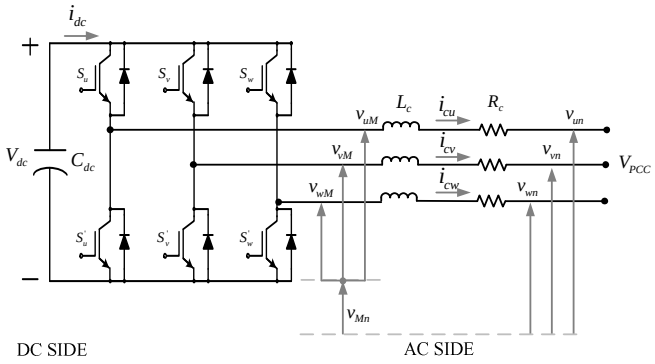

Fig. 3 The equivalent circuit of shunt active power filter

The circuit in Fig. 3 is the considered system used to derive the dynamic model of the shunt active power filter. On the AC side, the Kirchhoff's voltage law (KVL) is used to determine the three-phase voltage (v_{un},v_{vn},v_{wn}) at the PCC point as shown in (1)-(3).

$$v_{un} = L_c \frac{di_{cu}}{dt} + R_c i_{cu} + v_{uM} + v_{Mn} \tag{1}$$

$$v_{vn} = L_c \frac{di_{cv}}{dt} + R_c i_{cv} + v_{vM} + v_{Mn} \tag{2}$$

$$v_{wn} = L_c \frac{di_{cw}}{dt} + R_c i_{cw} + v_{wM} + v_{Mn} \tag{3}$$

The three-phase system in this work is the balanced three-phase three-wire system. This is the assumption to derive the mathematical model in the paper. Therefore, the summation of the three-phase voltages at the PCC point and the three-phase compensating currents are equal to zero as given in (4) and (5), respectively.

$$v_{un} + v_{vn} + v_{wn} = 0 \tag{4}$$

$$i_{cu} + i_{cv} + i_{cw} = 0 \tag{5}$$

In the steady state condition, substituting the three-phase voltage from (1)-(3) into (4) gives the relation in (6) as follows:

$$v_{Mn} = -\frac{1}{3}\sum_{k=u,v,w} v_{kM} \tag{6}$$

The relation of the input DC voltage (V_{dc}) and output three-phase voltages of the inverter (v_{uM},v_{vM},v_{wM}) is explained by (7). In this equation, k is equal to u, v and w for phase u, phase v and phase w, respectively. The c_k in (7) is the switching function of the IGBTs.

$$v_{kM} = c_k V_{dc} \tag{7}$$

Rearranging (1)-(3) using (6) and (7) obtains the differential equation of the three-phase compensating currents as shown by (8).

$$\frac{di_{ck}}{dt} = \frac{1}{L_c}v_{kn} - \frac{R_c}{L_c}i_{ck} - \frac{1}{L_c}d_{nk}V_{dc} \tag{8}$$

where the switching state function (d_{nk}) is explained by:

$$d_{nk} = (c_k - \frac{1}{3}\sum_{k=u,v,w} c_k) \tag{9}$$

On the DC side of the circuit in Fig. 3, the differential equation of the DC bus voltage across the capacitor (C_{dc}) is shown in (10).

$$\frac{dV_{dc}}{dt} = \frac{1}{C_{dc}}i_{dc} = \frac{1}{C_{dc}}\sum_{k=u,v,w} c_k i_{ck} = \frac{1}{C_{dc}}\sum_{k=u,v,w} d_{nk} i_{ck} \tag{10}$$

The dynamic model of the shunt active power filter on three-phase system in term of the state variable model can be written by (11).

$$\frac{d}{dt}\begin{bmatrix} i_{cu} \\ i_{cv} \\ i_{cw} \\ V_{dc} \end{bmatrix} = \begin{bmatrix} -\frac{R_c}{L_c} & 0 & 0 & -\frac{d_{nu}}{L_c} \\ 0 & -\frac{R_c}{L_c} & 0 & -\frac{d_{nv}}{L_c} \\ 0 & 0 & -\frac{R_c}{L_c} & -\frac{d_{nw}}{L_c} \\ \frac{d_{nu}}{C_{dc}} & \frac{d_{nv}}{C_{dc}} & \frac{d_{nw}}{C_{dc}} & 0 \end{bmatrix}\begin{bmatrix} i_{cu} \\ i_{cv} \\ i_{cw} \\ V_{dc} \end{bmatrix} + \frac{1}{L_c}\begin{bmatrix} v_{un} \\ v_{vn} \\ v_{wn} \\ 0 \end{bmatrix} \tag{11}$$

In this paper, the DQ approach is used to describe the control strategy of the system. Therefore, the mathematical model on three-phase system in (11) can be transformed into the DQ frame using the transformation matrix by (12). The f_u, f_v, and f_w are the current or voltage on three-phase system while the f_d and f_q are the current or voltage on DQ frame. The transformation matrix (K) in (12) is shown in (13). On the other hand, the DQ frame values can transform to the three-phase values using (14). The θ in matrix K is the phase angle of the source voltage vector as shown in the vector diagram of Fig. 4. In the paper, we set the d-axis on the source voltage vector with the same phase angle.

$$\begin{bmatrix} f_d \\ f_q \end{bmatrix} = K \cdot \begin{bmatrix} f_u \\ f_v \\ f_w \end{bmatrix} \tag{12}$$

$$K = \sqrt{\frac{2}{3}}\begin{bmatrix} \cos(\theta) & \cos(\theta + \frac{2\pi}{3}) & \cos(\theta - \frac{2\pi}{3}) \\ -\sin(\theta) & -\sin(\theta + \frac{2\pi}{3}) & -\sin(\theta - \frac{2\pi}{3}) \end{bmatrix} \tag{13}$$

$$\begin{bmatrix} f_u \\ f_v \\ f_w \end{bmatrix} = K^{-1} \cdot \begin{bmatrix} f_d \\ f_q \end{bmatrix} \tag{14}$$

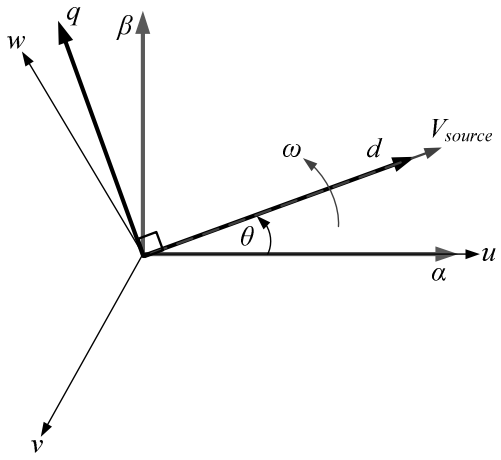

Fig. 4 The vector diagram of the DQ frame

From (11), the differential equation of the compensating current on three-phase frame can be transformed to the DQ frame using (12) and (14) as given in (15). Rearranging (15) obtains (16).

$$\frac{d[K^{-1}]\begin{bmatrix} i_{cd} \\ i_{cq} \end{bmatrix}}{dt} = \frac{1}{L_c}\begin{bmatrix} 1 & 0 \\ 0 & 1 \end{bmatrix}\cdot\left([K^{-1}]\begin{bmatrix} v_{dn} \\ v_{qn} \end{bmatrix}\right) - \frac{R_c}{L_c}\begin{bmatrix} 1 & 0 \\ 0 & 1 \end{bmatrix}\cdot\left([K^{-1}]\begin{bmatrix} i_{cd} \\ i_{cq} \end{bmatrix}\right) - \frac{1}{L_c}\begin{bmatrix} 1 & 0 \\ 0 & 1 \end{bmatrix}\cdot\left([K^{-1}]\begin{bmatrix} d_{nd}V_{dc} \\ d_{nq}V_{dc} \end{bmatrix}\right) \quad (15)$$

$$\frac{d}{dt}\begin{bmatrix} i_{cd} \\ i_{cq} \end{bmatrix} = \begin{bmatrix} \frac{1}{L_c} & 0 \\ 0 & \frac{1}{L_c} \end{bmatrix}\cdot\left(\begin{bmatrix} v_{dn} \\ v_{qn} \end{bmatrix}\right) - \begin{bmatrix} \frac{R_c}{L_c} & -\omega \\ \omega & \frac{R_c}{L_c} \end{bmatrix}\cdot\left(\begin{bmatrix} i_{cd} \\ i_{cq} \end{bmatrix}\right) - \begin{bmatrix} \frac{1}{L_c} & 0 \\ 0 & \frac{1}{L_c} \end{bmatrix}\cdot\left(\begin{bmatrix} d_{nd}V_{dc} \\ d_{nq}V_{dc} \end{bmatrix}\right) \quad (16)$$

From (11), the differential equation of the DC bus voltage can be transformed to the DQ frame as shown in (17).

$$\frac{dV_{dc}}{dt} = \frac{1}{C_{dc}}\left([K^{-1}]^T\begin{bmatrix} d_{nd} \\ d_{nq} \end{bmatrix}\right)\cdot\left([K^{-1}]\begin{bmatrix} i_{cd} & i_{cq} \end{bmatrix}\right) \quad (17)$$

Rearranging (17) obtains (18).

$$\frac{dV_{dc}}{dt} = \frac{1}{C_{dc}}\begin{bmatrix} d_{nd} \\ d_{nq} \end{bmatrix}\cdot\begin{bmatrix} i_{cd} & i_{cq} \end{bmatrix} \quad (18)$$

From (16) and (18), the dynamic model of the shunt active power filter on DQ frame in term of the state variable model can be written by (19).

$$\frac{d}{dt}\begin{bmatrix} i_{cd} \\ i_{cq} \\ V_{dc} \end{bmatrix} = \begin{bmatrix} -\frac{R_c}{L_c} & \omega & -\frac{d_{nd}}{L_c} \\ -\omega & -\frac{R_c}{L_c} & -\frac{d_{nq}}{L_c} \\ \frac{d_{nd}}{C_{dc}} & \frac{d_{nq}}{C_{dc}} & 0 \end{bmatrix}\begin{bmatrix} i_{cd} \\ i_{cq} \\ V_{dc} \end{bmatrix} + \frac{1}{L_c}\begin{bmatrix} v_{dn} & 0 \\ 0 & v_{qn} \\ 0 & 0 \end{bmatrix} \quad (19)$$

IV. The Design of Current Loop Controllers and Control Strategy

In the paper, the PI controllers are used to control the compensating currents of the shunt active power filter for harmonic elimination in the system. The PI controllers design and the control strategy of current loop based on the dynamic model on DQ frame is presented in this section. From (19), the differential equations of the compensating current on DQ frame are explained by (20) and (21).

$$L_c\frac{di_{cd}}{dt} + R_c i_{cd} = \omega L_c i_{cq} - d_{nd}V_{dc} + v_{dn} \quad (20)$$

$$L_c\frac{di_{cq}}{dt} + R_c i_{cq} = -\omega L_c i_{cd} - d_{nq}V_{dc} + v_{qn} \quad (21)$$

The output voltages of the voltage source inverter represented as the shunt active power filter on DQ frame (v_{dl} and v_{ql}) are shown by (22) and (23).

$$v_{dl} = d_{nd}V_{dc} \quad (22)$$

$$v_{ql} = d_{nq}V_{dc} \quad (23)$$

Substituting v_{dl} and v_{ql} to (20) and (21) gives the voltage at PCC point on DQ frame as shown by (24) and (25).

$$v_{dn} = R_c i_{cd} + L_c\frac{di_{cd}}{dt} - \omega L_c i_{cq} + v_{dl} \quad (24)$$

$$v_{qn} = R_c i_{cq} + L_c\frac{di_{cq}}{dt} + \omega L_c i_{cd} + v_{ql} \quad (25)$$

On the DQ frame, the voltage on d-axis and q-axis at PCC point are equal to $|V|$ and 0, respectively.

$$|V| = R_c i_{cd} + L_c\frac{di_{cd}}{dt} - \omega L_c i_{cq} + v_{dl} \quad (26)$$

$$0 = R_c i_{cq} + L_c\frac{di_{cq}}{dt} + \omega L_c i_{cd} + v_{ql} \quad (27)$$

From (26) and (27), the reference voltages of the shunt active power filter on DQ frame (v_{dl}^*, v_{ql}^*) are shown in (28) and (29).

$$v_{dl}^* = \omega L_c i_{cq} - u_d + |V| \quad (28)$$

$$v_{ql}^* = -\omega L_c i_{cd} - u_q \quad (29)$$

The output signals of plant on d-axis and q-axis (u_d, u_q) are shown in (30) and (31), respectively.

$$u_d = L_c\frac{di_{cd}}{dt} + R_c i_{cd} \quad (30)$$

$$u_q = L_c \frac{di_{cq}}{dt} + R_c i_{cq} \tag{31}$$

From (28) and (29), the control strategy of the compensating currents of the shunt active power filter is depicted in Fig. 1. The plants to design the PI controllers for two current loops can derive from (30) and (31) by using Laplace transform as shown in (32).

$$\frac{I_{cd}}{U_d} = \frac{I_{cq}}{U_q} = \frac{1}{L_c s + R_c} \tag{32}$$

From Fig. 1, the transfer functions of the PI controllers on d-axis and q-axis can derive from (33) and (34), respectively.

$$u_d = K_{PC}\tilde{i}_d + K_{IC}\int \tilde{i}_d dt \tag{33}$$

$$u_q = K_{PC}\tilde{i}_q + K_{IC}\int \tilde{i}_q dt \tag{34}$$

From (33) and (34), the transfer functions of the PI controllers on DQ frame are shown in (35).

$$\frac{U_d}{\tilde{I}_d} = \frac{U_q}{\tilde{I}_q} = \frac{(K_{PC}s + K_{IC})}{s} \tag{35}$$

From (32) and (35), the block diagrams for the PI controllers design on DQ frame are depicted in Fig. 5.

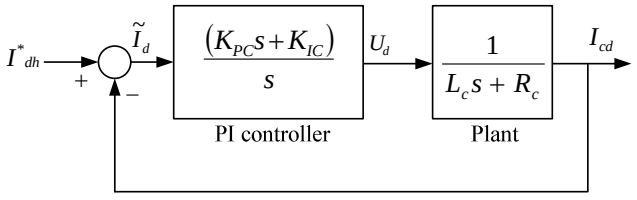

(a) Current loop of d-axis

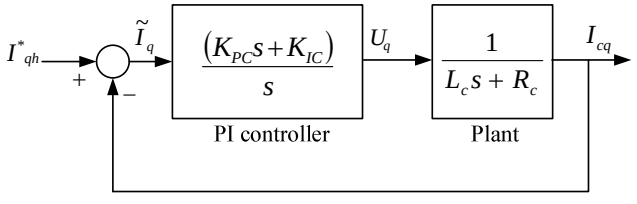

(b) Current loop of q-axis

Fig. 5 The block diagram to design the PI controllers on DQ frame for two current loops

From the block diagram in Fig. 5, the closed-loop transfer functions on DQ frame are shown in (36).

$$\frac{I_{cd}}{I^*_{dh}} = \frac{I_{cq}}{I^*_{qh}} = \frac{K_{PC}}{L_c}\left(\frac{s + \frac{K_{IC}}{K_{PC}}}{s^2 + (\frac{R_c + K_{PC}}{L_c})s + \frac{K_{IC}}{L_c}}\right) \tag{36}$$

Equation (36) is used to compare with the standard second order characteristic equation as shown in (37).

$$G(s) = \frac{\omega_{ni}^2}{s^2 + 2\xi\omega_{ni}s + \omega_{ni}^2} \tag{37}$$

Comparing (36) with (37), the K_{PC} and K_{IC} of the PI controllers can be calculated from (38) and (39), respectively.

$$K_{PC} = 2\xi\omega_{ni}L_c - R_c \tag{38}$$

$$K_{IC} = \omega_{ni}^2 L_c \tag{39}$$

The damping ratio (ξ) in (38) is defined to 0.707. The natural frequency (ω_{ni}) equal to 5000π rad/s because of the harmonic order considered in the system is set to 50. The resistance (R_c) of the shunt active power filter is neglect while the inductance (L_c) is set to 39 mH from Table 1. Substituting all values in (38) and (39) gives K_{PC}= 866 and K_{IC} = 9.62×10^6.

V. The Design of Voltage Loop Controller

The differential equation of the DC bus voltage and current in Fig. 3 on DQ frame are shown in (40) and (41), respectively.

$$\frac{dV_{dc}}{dt} = \frac{d_{nd}}{C_{dc}} i_{cd} + \frac{d_{nq}}{C_{dc}} i_{cq} \tag{40}$$

$$i_{dc} = C_{dc}\frac{d}{dt}V_{dc} \tag{41}$$

Substituting i_{dc} from (41) to (40) gives the relation in (42).

$$i_{dc} = d_{nd} i_{cd} + d_{nq} i_{cq} \tag{42}$$

The plant for design the PI controller of voltage loop can derive from (41) by using Laplace transform as shown in (43).

$$\frac{V_{dc}}{I_{dc}} = \frac{1}{C_{dc}s} \tag{43}$$

From Fig. 1., the output of the PI controller can be described by (44). Therefore, the transfer function of the PI controller for voltage loop is shown in (45).

$$i_{dv} = K_{PV}\tilde{v}_{dc} + K_{IV}\int \tilde{v}_{dc}dt \tag{44}$$

$$\frac{I_{dv}}{\tilde{V}_{dc}} = \frac{\left(K_{PV}s + K_{IV}\right)}{s} \tag{45}$$

From Fig. 3, the AC side power is equal to the DC side power as shown in (46). The losses in capacitor, resistor and inductor are neglect as the condition of this equation.

$$V_{dc}i_{dc} = v_{dn}i_{cd} + v_{qn}i_{cq} \tag{46}$$

In the paper, the PWM technique is used to generate the switching signals. The power conserving convention of the DQ transformation is also used. Therefore, (46) can be rewritten as shown in (47). The *m* in this equation is the modulation index of the desired operating point.

$$V_{dc}i_{dc} = \frac{\sqrt{3}m}{2\sqrt{2}}V_{dc}i_{dv} \tag{47}$$

Taking Laplace transform in (47) gives (48).

$$\frac{I_{dc}}{I_{dv}} = \frac{\sqrt{3}m}{2\sqrt{2}} \tag{48}$$

From (43), (45) and (48), the block diagram using for the PI controller design of the DC bus voltage control is depicted in Fig. 6.

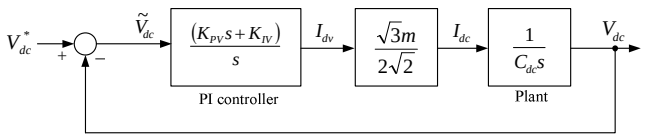

Fig. 6 The block diagram to design the PI controller for voltage loop

From the block diagram in Fig. 6, the closed-loop transfer function is shown in (49).

$$\frac{V_{dc}}{V_{dc}^*} = \frac{\sqrt{3}m}{2\sqrt{2}}\frac{1}{C_{dc}}\left(\frac{K_{PV}s + K_{IV}}{s^2 + (\frac{\sqrt{3}m}{2\sqrt{2}}\frac{K_{PV}}{C_{dc}})s + \frac{\sqrt{3}m}{2\sqrt{2}}\frac{K_{IV}}{C_{dc}}}\right) \tag{49}$$

Equation (49) is used to compare with the standard second order characteristic equation as shown in (37). From this comparison, the K_{PV} and K_{IV} of the PI controller can be calculated from (50) and (51), respectively.

$$K_{PV} = \frac{4\sqrt{2}\xi\omega_{nv}C_{dc}}{\sqrt{3}m} \tag{50}$$

$$K_{IV} = \frac{2\sqrt{2}\omega_{nv}^2 C_{dc}}{\sqrt{3}m} \tag{51}$$

The capacitor value of the shunt active power filter is set to 200 μF from Table 1. The damping ratio still be set to 0.707. The natural frequency of the voltage loop (ω_{nv}) is set to 10π rad/s in this paper. The DC bus voltage command (V_{dc}^*) is set to 750 V. Therefore, the modulation index (*m*) is equal to 0.83. Substituting all values in (50) and (51) obtains K_{PV} = 0.0175 and K_{IV} = 0.3884.

VI. Simulation Results and Discussions

The simulation results of the system in Fig. 1 with the system parameters from Table I are depicted in Fig. 7. In the paper, the average total harmonic distortion ($\%THD_{av}$) is used as the performance index for the harmonic mitigation. The $\%THD_{av}$ can be calculated by (52). In Fig. 7, the source currents before compensation (i_{Lu}, i_{Lv}, i_{Lw}) are highly distorted waveform. From Table II, the $\%THD_{av}$ of the source currents before compensation is equal to 24.42%. This value is extremely greater than the IEEE Std. 519-1992. When the shunt active power filter injects the compensating currents (i_{cu}, i_{cv}, i_{cw}), the source currents (i_{su}, i_{sv}, i_{sw}) are nearly sinusoidal waveform. The $\%THD_{av}$ of these currents after compensation is equal to 1.69% that is satisfied under IEEE Std. 519-1992.

$$\%THD_{av} = \sqrt{\frac{\sum_{k=u,v,w}\%THD_k^2}{3}} \tag{52}$$

TABLE I
System Parameters

Line voltage and frequency	V_s=312 V(peak), f_s=50 Hz
Line impedance	L_s=0.1 mH
Three – phase diode rectifiers parameters	$L_{L,max}$=4 H, $R_{L,max}$ =130 Ω $L_{L,min}$=2 H, $R_{L,min}$ =65 Ω
Shunt active power filter parameters	L_c=39 mH, C_{dc}=200μF
Switching frequency	f_{sw}=5000 Hz
Current loop controllers parameters	K_{PC} =866 , K_{IC} =9.62×10^6
Voltage loop controller parameters	K_{PV} =0.0175 , K_{IV} =0.3884

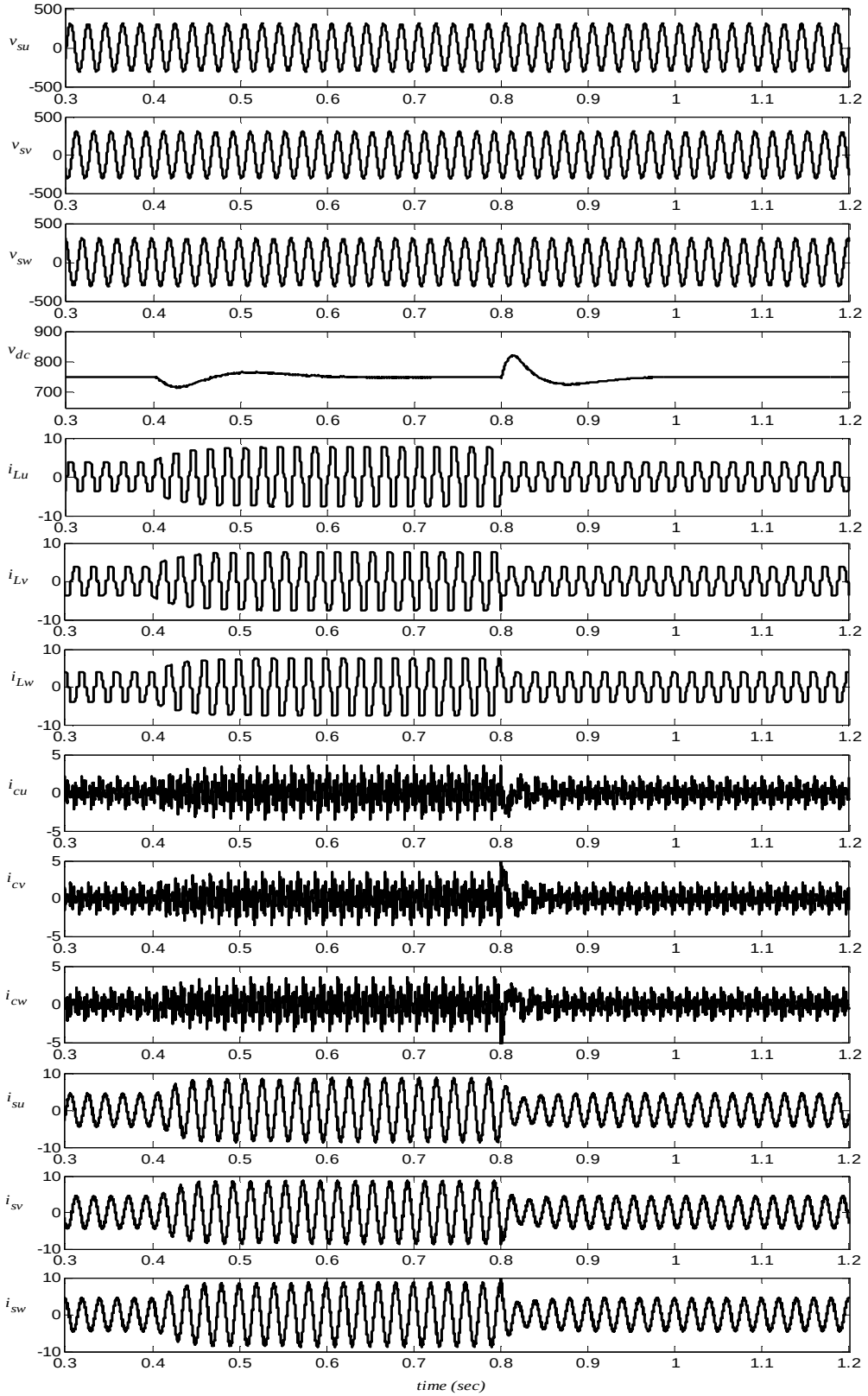

Fig. 7 The simulation results

TABLE II
%THD OF THE SOURCE CURRENTS BEFORE AND AFTER COMPENSATION

phase	%THD of the source currents	
	%THD before compensation	%THD after compensation
u	24.42	1.67
v	24.42	1.70
w	24.42	1.71
$\%THD_{av}$	24.42	1.69

From Fig. 1, the load impedance of the three-phase bridge rectifier is changed at t = 0.4 – 0.8 s. Therefore, the amplitude of source currents at this period increases. The shunt active power filter can still compensate the harmonic current even though the load is varied. From Fig. 8, it confirms that the PI controllers of two current loops can control the compensating currents to track the reference currents (i^*_{cu}, i^*_{cv}, i^*_{cw}). In this paper, the reference currents can be calculated from the DQF method. Moreover, the DC bus voltage is still constant at 750 V as shown in Fig. 7. For this reason, the PI controller of the voltage loop can regulate the DC bus voltage.

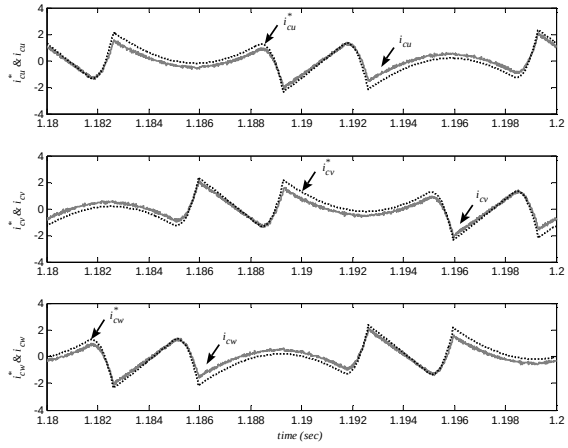

Fig. 8 The compensating and reference currents of the system

VII. CONCLUSION

This paper presents how to derive the mathematical model of the shunt active power filter on DQ frame. The pulse width modulation (PWM) technique is applied to generate the switching signals of the shunt active power filter. The voltage source inverter (VSI) is used as the shunt active power filter. The PI controllers are applied to control the injection of the compensating currents and the DC bus voltage following on the command value. The design method of these controllers is completely presented in the paper. Moreover, the overall control strategy of the system on DQ frame is also presented. In the paper, the DQF method is used to calculate the reference currents of the shunt active power filter. The simulation results show that the control strategy and the design method presented in the paper can provide the good performance of the shunt active power filter. Furthermore, the %THD of the source currents after compensation can follow the IEEE Std.519-1992 and these waveforms are nearly sinusoidal.

ACKNOWLEDGMENT

This work was supported by Suranaree University of Technology (SUT) and by the office of the Higher Education Commission under NRU project of Thailand.

REFERENCES

[1] Indrajit P. and Paul J.S., "Effect of Harmonic on Power Measurement," *IEEE Petroleum and Chemical Industry Conference*, 1989, pp. 129 – 132.
[2] Elham B.M., Clarence L.W., and Adly A.G., "A Harmonic Analysis of the Induction Watthour Meter's Registration Error," *IEEE Transaction on Power Delivery*, vol. 7, no. 3, 1992, pp. 1080 – 1088.
[3] Ho J.M., Liu C.C., "The Effects of Harmonics on Differential Relay for a Transformer," *IEEE International Conference and Exhibition on Electricity Distribution (CIRED)*, vol.2, 2001.
[4] IEEE Std. 519 – 1992, IEEE Recommended practices and requirement for harmonic control in electrical power system.
[5] Peng, F. Z., Akagi, H., and Nabae, A., "A New Approach to Compensation in Power Systems," *Industry Applications Society Annual Meeting., Conference Record of the 1988 IEEE*, vol. 1, Oct 1988, pp. 874-880.
[6] Peng F. Z. and Lai J-S, 1996 , "Generalized instantaneous reactive power theory for threephase power system" *IEEE Trans. Instrum. Meas*.,vol.45, no.1, February, pp. 293-297.
[7] B. Zhang, "The Method based on a Generalized dqk Coordinate Transform for Current Detection of an Active Power Filter and Power System", *IEEE Power Electronics Specialists Conference*, 2007, pp. 242- 248.
[8] Chang, G.W. and Chen, S.K., "An a-b-c Reference Frame-Based Control Strategy for the Three-Phase Four-Wire Shunt Active Power Filter," *IEEE International Conference on Harmonics and Quality of Power*, vol. 1, pp. 26-29.
[9] Chen, C.L., Lin, C.E. and Huang, C.L., "An Active Filter for Unbalanced Three-Phase System Using Synchronous Detection Method," *IEEE Conference on Power Electronics Specialists 1994 (PESC '94)*, vol. 2, pp. 1451-1455.
[10] Sujitjorn, S., Areerak, K.-L. and Kulworawanichpong, T., "The DQ Axis With Fourier (DQF) Method for Harmonic Identification," *IEEE Transactions on Power Delivery*, vol. 22, no. 2, pp. 737-739, Jan. 2007.
[11] Zeng J., Yu C. ,Qi Q., Yan Z., Ni Y., Zhang B.L.,Chen S., and Wu F. F., "A Novel Hysteresis Current Control for Active Power Filter with Constant Frequency," *Electric Power Systems Research 68*, pp.75- 82, Jan. 2004.
[12] Kazmierkowski M.P. and Dzieniakowski, M.A. (1993). "Review of current regulation methods for VS-PWM inverters," *IEEE International Symposium on Industrial Electronics 1993 (ISIE '93)*, pp. 448–456.
[13] P. Prasomsak, Kongpol Areerak, Kongpan Areerak, and A. Srikaew, "Control of Shunt Active Power Filters using Fuzzy Logic Controller," *The IASTED International Conference Modeling, Identification, and Control (AsiaMIC 2010)*, Thailand, pp. 107-113, Nov. 2010.
[14] N. Mendalek, K. AI-Haddad, F. Fnaiech and L.A. Dessaint, "Nonlinear control technique to enhance dynamic performance of a shunt active power filter," in *IEE Proc. Electric Power Applications*, vol.150, no.4, pp. 373–379, July 2003.
[15] M. EI-Habrouk and M. K. Darwish, "Design and implementation of a modified Fourier analysis harmonic current computation technique for power active filter using DSPs," *Proc. Inst. Elect. Eng., Elect. Power Appl.*, vol. 148, no. 1, pp. 21–28, Jan. 2001.
[16] Areerak, K.-L., "Harmonic Detection Algorithm based on DQ Axis with Fourier Analysis for Hybrid Power Filters," *WSEAS TRANSACTIONS on POWER SYSTEMS*, vol. 3, no. 11, pp.665-674, Nov. 2008.

P. Santiprapan was born in Ranong, Thailand, in 1988. He received the B.S. degree in electrical engineering from Suranaree University of Technology (SUT), Nakhon Ratchasima, Thailand, in 2009, where he is currently studying toward the M.Eng. degree in electrical engineering. His main research interests include the shunt active power filter, harmonic elimination, artificial intelligence applications, simulation and modeling.

K-L. Areerak received the B.Eng, M.Eng, and Ph.D. degrees in electrical engineering from Suranaree University of Technology (SUT), Thailand, in 2000, 2003, and 2007, respectively. Since 2007, he has been a lecturer and Head of Power Quality Research Unit (PQRU) in the School of Electrical Engineering, SUT. He received the Assistant Professor in Electrical Engineering in 2009. His main research interests include active power filter, harmonic elimination, artificial intelligence applications, motor drive, and intelligence control systems.

K-N. Areerak received the B.Eng. and M.Eng degrees from Suranaree University of Technology (SUT), Nakhon Ratchasima, Thailand, in 2000 and 2001, respectively and the Ph.D. degree from the University of Nottingham, Nottingham, UK., in 2009, all in electrical engineering. In 2002, he was a lecturer in the Electrical and Electronic Department, Rangsit University, Thailand. Since 2003, he has been a Lecturer in the School of Electrical Engineering, SUT. His main research interests include system identifications, artificial intelligence applications, stability analysis of power systems with constant power loads, modeling and control of power electronic based systems, and control theory.